where

λ_{g1} = guide wavelength of TE_{10}□

X = distance from the center of the slot to the end plate of the cavity

$$M_1 = \frac{\pi l^3}{24\left(\log_e \frac{4l}{w} - 1\right)},$$

$$\alpha_1 = 2.728 \frac{t_1}{l} \sqrt{1 - \left(\frac{2l}{\lambda}\right)^2}$$

l, w = length and width of the slot which has an approximately elliptic shape ($l \gg w$)

t_1 = depth of the slot

a, b = inner dimensions of the rectangular guide

R = radius of the cavity

R' = radius of the output circular guide which corresponds to the inside radius of the slidable pipe in Fig. 5(a)

λ_{g2}' = guide wavelength in the output circular guide

$$M_2 = \frac{4}{3} r^3, \quad \alpha_2 = 3.200 \frac{t_2}{2r} \sqrt{1 - \left(1.706 \frac{2r}{\lambda}\right)^2}$$

r = radius of the circular hole in coupling plate "2"

ρ = position of the circular hole [see Fig. 5(b)]

t_2 = depth of the circular hole.

ACKNOWLEDGMENT

The author wishes to thank Prof. K. Suetake, Tokyo Institute of Technology, for his valuable discussions, and Dr. I. Sekiguchi, Hitachi Central Research Lab., for his constant encouragement.

REFERENCES

[1] B. Oguchi and K. Yamaguchi, "Centre-excited type of rectangular TE_{10} to circular TE_{01} mode transducer," *Proc. IEE*, vol. 106, pt. B, suppl. 13, p. 132–137, January 1959.
[2] G. C. Southworth, *Principles and Applications of Waveguide Transmission*. Princeton, N. J.: Van Nostrand, p. 362.
[3] P. H. Wolfert, "A wide-band rectangular-to-circular mode transducer for millimeter waves," *IEEE Trans. on Microwave Theory and Techniques (Correspondence)*, vol. MTT-11, pp. 430–431, September 1963.
[4] S. E. Miller, "Coupled wave theory and waveguide applications," *Bell Sys. Tech. J.*, vol. 33, p. 661–719, May 1954.
[5] A. Jaumann, "Über Richtungskoppler zur Erzeugung der H_{01}-Welle im Runden Hohlleiter," *Arch. elekt. Übertragung*, vol. 12, p. 440–446, October 1958.
[6] D. A. Lanciani, "H_{01} mode circular waveguide components," *IRE Trans. on Microwave Theory and Techniques*, vol. MTT-2, pp. 45–51, July 1954.
[7] K. Noda, "Mode exciters in circular waveguides," *Rev. Elec. Commun. Lab. (Japan)*, vol. 8, p. 465–476, September–October 1960.
[8] S. Shimada, "Resonant cavity type mode transducer," *1961 Nat'l Conv. Rec. IECE of Japan*, no. 196, November 1961.
[9] ——, "Resonant cavity type mode transducer and mode filter for the circular TE_{02} mode," Millimeter and Submillimeter Conf., Orlando, Fla., January 1963.
[10] ——, "Resonant cavity type TE_{10}□-TE_{01}○ mode transducer," *J. IECE of Japan*, vol. 48, p. 1206–1215, July 1965.
[11] ——, "Circular wavequide components at millimeter wavelength-mode transducers," *Hitachi, Rev.* (Japan), to be published.
[12] ——, "Mode transducers in the 50 Gc/s region," rept. of the research committee on millimeter waves in Japan, pp. 62–64. Japan: Corona, 1963.
[13] C. G. Montgomery, *Principles of Microwave Circuits*. New York: McGraw-Hill, ch. 2.
[14] H. A. Bethe, "Theory of diffraction by small holes," *Phys. Rev.*, vol. 66, p. 163–182, 1944.

Dispersion Characteristics of an Array of Parasitic Linear Elements

E. R. NAGELBERG, MEMBER, IEEE, AND J. SHEFER, SENIOR MEMBER, IEEE

Abstract—**In this paper we study the properties of a transmission line consisting of an infinite array of conducting cylinders, placing emphasis on the dispersion characteristics of the lowest order slow wave mode. We present experimental results for the variation of phase velocity with frequency, and then, using a method of parameter estimation, determine the element current distribution which best explains these observations. Assuming this distribution to be of the form**

$$j(x; \gamma) = j_0 \left[1 - \left(\frac{|x|}{h}\right)^{\gamma}\right],$$

we find that, for a given size of element, there is a value of γ which gives very good agreement for the variation of phase velocity over the frequency range of interest.

Manuscript received March 18, 1966; revised May 2, 1966.
The authors are with Bell Telephone Laboratories, Inc., Whippany, N. J.

I. INTRODUCTION

IN THE FOLLOWING we study certain characteristics of an infinitely long, uniform array of conducting cylinders, as illustrated in Fig. 1. This structure can support a guided wave which travels along the axis with a phase velocity less than the velocity of light. The propagation characteristics of this slow wave are of interest for two reasons. First, the results may be applied to analysis of the Yagi antenna, which can be thought of

as a slow wave structure terminated in free space [1]. Furthermore, it has been observed that such an array functions very well as a microwave transmission line [2] with frequency and loss characteristics comparable to a conventional waveguide.

Referring again to Fig. 1, we denote the direction of propagation as the z direction, with transverse coordinates labeled x and y, the x direction being parallel to the elements. The pertinent geometrical parameters are the element half-length h, the cylinder radius a, and the interelement spacing d.

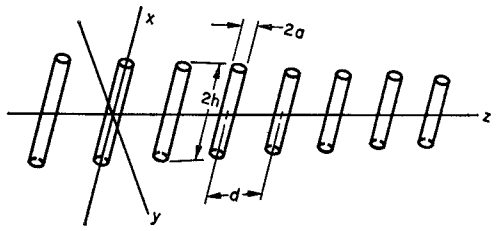

Fig. 1. Array of parasitic elements showing coordinate system.

It is clear that the characteristics of this array will be a function of the element current distributions. These are very difficult to determine, either analytically or experimentally, so that in previous analyses of this structure [1], [3], the calculations have been based on some apriori assumption for the current. An example of such an assumed variation would be the "shifted cosine" distribution,

$$j(x) = j_0\left(\frac{\cos kx - \cos kh}{1 - \cos kh}\right), \tag{1}$$

which is the zero-order solution to Hallen's integral equation for a single thin linear antenna [1], [4].

In what follows we describe an approach in which we use the measured dispersion characteristics of the array in order to deduce the element current distribution. This is carried out out by a method of parameter estimation in which we utilize a digital computer to determine that member of a one-parameter family of current distributions which best predicts the observed variation of phase velocity of the slow wave as a function of frequency. This set of curves is chosen to be of the form

$$j(x;\gamma) = j_0\left[1 - \left(\frac{|x|}{h}\right)^{\gamma}\right] \tag{2}$$

where the parameter γ has been introduced to account for the change in current distribution with element thickness. We will show that for a given size of element there exists a value of γ which gives very good agreement over the frequency range of interest.

The paper is organized as follows. In Section II we present the basic analysis and derive the dispersion equation for the current distribution of (2). Section III describes the experimental techniques used for the phase velocity measurements, together with the results of estimating γ for cylinders with different radii. Then, in Section IV, we give an approximate analysis of the dispersion equation, corresponding to the case where the slow wave velocity is close to the free space velocity.

The formulas will be expressed in terms of rationalized MKS units, using the (suppressed) harmonic time dependence $e^{-i\omega t}$.

II. Derivation of the Dispersion Equation

As the guided wave propagates along the array, currents are induced in the elements, the current in any element differing from that in its nearest neighbors only by the phase factor $e^{i\beta d}$, where β is the slow wave propagation constant. The current density corresponding to the nth element is therefore

$$J_n(x, y, z) = e_x j(x) e^{i\beta nd}\delta(y)\delta(z - nd) \tag{3}$$

where e_x is a unit vector in the x direction and $j(x)$ is the amplitude distribution function. In using a delta function dependence on y and z we make the reasonable assumption that the contribution to the electromagnetic field due to each element may be lumped in an equivalent filamentary current located on the axis of the cylinder. The total current J is the sum over all elements and is given by

$$J = \sum_{n=-\infty}^{+\infty} J_n = e_x j(x)\delta(y) \sum_{n=-\infty}^{+\infty} e^{i\beta nd}\delta(z - nd). \tag{4}$$

The vector potential $\boldsymbol{A}$ may then be calculated using the free space Green's function, with the result that[1]

$$\boldsymbol{A}(x, y, z) = e_x \frac{\mu_0}{4\pi} \sum_{n=-\infty}^{+\infty} e^{i\beta nd} \cdot \int_{x'=-h}^{+h} j(x') \frac{\exp[ik\sqrt{(x - x')^2 + y^2 + (z - nd)^2}]}{\sqrt{(x - x')^2 + y^2 + (z - nd)^2}} dx'. \tag{5}$$

In order to elicit the guided wave character of the field, we next transform the vector potential into its spatial frequency representation. This equivalent description is obtained from (5) by applying the Poisson summation formula [5]

$$\sum_{n=-\infty}^{n+\infty} f(nd) = \frac{1}{d} \sum_{m=-\infty}^{+\infty} \mathfrak{F}\left(\frac{2\pi m}{d}\right) \tag{6}$$

where $\mathfrak{F}$ denotes the exponential Fourier transform of the function f; i.e.,

$$\mathfrak{F}(\zeta) = \int_{-\infty}^{+\infty} f(u) e^{-i\zeta u} du. \tag{7}$$

[1] The Lorentz gauge is used throughout.

In particular, for the function appearing in (5), namely

$$f(u) = \frac{\exp[i\beta u + ik\sqrt{(x-x')^2+(y-y')^2+(z-u)^2}]}{\sqrt{(x-x')^2+(y-y')^2+(z-u)^2}}, \quad (8)$$

it is found that [6]

$$\mathfrak{F}(\zeta) = 2e^{i\beta z}e^{i\zeta z}K_0(\alpha\sqrt{(x-x')^2+(y-y')^2}),$$

$$-\frac{\pi}{2} < \arg\alpha < \frac{\pi}{2} \quad (9)$$

where K_0 denotes the modified Bessel function of the second kind and α is given by

$$\alpha = \sqrt{(\beta-\zeta)^2 - k^2}. \quad (10)$$

We thus obtain the spatial frequency representation for the vector potential,

$$\boldsymbol{A}(x, y, z) = \boldsymbol{e}_x \frac{\mu_0}{2\pi d} e^{i\beta z} \sum_{m=-\infty}^{+\infty} e^{-i(2m\pi/d)} \cdot \int_{x'=-h}^{h} j(x')K_0[\alpha_m\sqrt{(x-x')^2+y^2}]dx', \quad (11)$$

where

$$\alpha_m = \sqrt{\left(\beta - \frac{2m\pi}{d}\right)^2 - k^2}. \quad (12)$$

Observe that the right-hand side of (11) has the form predicted by Floquet's theorem [17] since it consists of a traveling-wave term $e^{i\beta z}$ multiplied by a complex periodic function with the same period as the structure. Also to be expected is the appearance of the modified Bessel function K_0, which decreases exponentially at large distances, describing a bound wave with no energy flow in the transverse plane. Of course, this requires that $\alpha_m > 0$, which falls within the restriction of (9).

The electric field may be derived from the vector potential using the familiar formula

$$\boldsymbol{E} = i\omega\boldsymbol{A} + \frac{1}{k^2}\nabla(\nabla\cdot\boldsymbol{A}). \quad (13)$$

In particular, since $\boldsymbol{A}$ has only one component, $\boldsymbol{A}_x$, the electric field parallel to the elements, E_x, is given by

$$E_x = i\omega\left(A_x + \frac{1}{k^2}\frac{\partial^2 A_x}{\partial x^2}\right). \quad (14)$$

We then substitute (11) into (14) and integrate by parts twice, taking advantage first of the symmetry of K_0 with respect to x and x', and second of the fact that the current distribution $j(x)$ vanishes at the ends of the elements [8]. The result for E_x is that

$$E_x = \frac{-i\omega\mu_0}{2\pi k^2 d} e^{i\beta z} \sum_{m=-\infty}^{+\infty} e^{-i(2m\pi/d)z} j'(x') K_0[\alpha_m\sqrt{(x-x_1)^2+y^2}]\Big|_{x'=-h}^{+h} - \int_{-h}^{+h} [j''(x') + k^2 j(x')] K_0[\alpha_m\sqrt{(x-x')^2+y^2}]dx'. \quad (15)$$

Setting $E_x = 0$ on the elements results in an integral equation involving $j''(x) + k^2 j$, in which the propagation constant β appears as a parameter. This equation is conveniently derived by transforming to a cylindrical coordinate system (ρ, ϕ, x) whose axis coincides with the element located at $z = 0$, as indicated in Fig. 2. The two coordinate systems are related by

$$y = \rho\cos\phi$$
$$z = \rho\sin\phi \quad (16)$$

with x common.

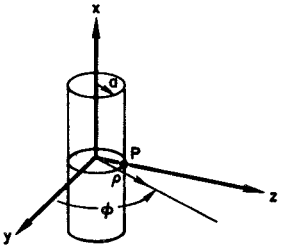

Fig. 2. Element located at $z = 0$ showing local coordinate representation.

The boundary conditions may then be satisfied by setting $|E_x| = 0$ at $\rho = a$. Clearly it follows that the electric field must vanish on all the elements, since the field amplitudes are periodic in the z direction with period d. The resulting integral equation, taking into account the even symmetry of $j(x)$, is given by

$$\sum_{m=-\infty}^{+\infty} e^{-i(2m\pi/d)\alpha\sin\phi} j'(h)[K_0(\alpha_m\sqrt{(x-h)^2+a^2\cos^2\phi}) + K_0(\alpha_m\sqrt{(x+h)^2+a^2\cos^2\phi})] - \int_{-h}^{+h} [j''(x') + k^2 j(x')] \cdot K_0(\alpha_m\sqrt{(x-x')^2+a^2\cos^2\phi})dx' = 0,$$
$$-h \le x \le +h \qquad 0 \le \phi \le 2\pi. \quad (17)$$

This equation could, in principle, be solved to yield the correct current density $j(x)$ and propagation constant β. However, since the complexity of (17) appears to preclude any straightforward solution for the current density, several simplifications are suggested.

First, as mentioned earlier, we assume a solution to (17) of the particular one-parameter form

$$j(x) = j_0\left[1 - \left(\frac{|x|}{h}\right)^{\gamma}\right] \tag{18}$$

where γ is yet to be determined. The class of distributions described by (18) includes many types which one would be led to assume as trial functions. These range from the triangular distribution, corresponding to $\gamma = 1$, to the uniform distribution, which is the limiting form of (18) as γ becomes very large. The parabolic case, $\gamma = 2$, is a good approximation, at least over the frequency range of interest here, to the so-called "shifted cosine" of (1).

As a further simplification, we satisfy the boundary condition at only one point on each element, the point designated as P in Fig. 2, having the coordinates $x = y = 0$, $z = a$. Since $|E_x|$ is an even function of x, y, and z, it follows that

$$\nabla |E_x| = 0 \quad \text{at} \quad x = y = z = 0. \tag{19}$$

Therefore, by setting $|E_x| = 0$ at P, we approximately satisfy this boundary condition at neighboring points on each element, both in the axial and peripheral directions.

Setting $x = y = 0$, $z = a$ in (15) and incorporating the assumed current distribution of (18), one can then derive the appropriate dispersion relation, which in this case is the characteristic equation for the propagation constant β. However, considerable complexity in the calculation can be avoided by exploiting the relative values of various geometrical parameters and wavelengths for the particular array and frequencies which are of interest. We shall thus assume for our purposes that

$$\beta a \ll 1, \tag{20}$$

$$\alpha_m h \gg 1, \qquad |m| \geq 1, \tag{21}$$

and

$$\beta d \ll 2\pi, \tag{22}$$

in which case the characteristic equation may be written as

$$\frac{\xi^2}{u} I(u, 0) - \frac{\xi^2}{u^{\gamma+1}} I(u, \gamma) - \frac{\gamma(\gamma - 1)}{u^{\gamma-1}} I(u, \gamma - 2) + \gamma K_0(u) - A(\gamma) = 0 \tag{23}$$

where

$$\xi = kh$$

$$u = \xi \frac{\sqrt{1 - \left(\frac{v}{c}\right)^2}}{\frac{v}{c}}. \tag{24}$$

In (24), k is the free space wavenumber, and the ratio v/c is the ratio of the phase velocity of the slow wave to the velocity of light. The function $I(u, \nu)$ is a weighted integral of the modified Bessel function defined as

$$I(u, \nu) = \int_0^u x^{\nu} K_0(x)\, dx. \tag{25}$$

The dependence on the element radius a and interelement spacing d is contained in the term $A(\gamma)$ which is defined as

$$A(\gamma) = \gamma(\gamma - 1) 2^{\gamma-2} \left(\frac{d}{2\pi h}\right)^{\gamma-1} \Gamma^2\left(\frac{\gamma - 1}{2}\right) \sum_{n=1}^{\infty} \frac{\cos n\left(\frac{2\pi a}{d}\right)}{n^{\gamma-1}} + \xi^2 \left(\frac{d}{4h}\right) \log\left[2 - 2\cos\left(\frac{2\pi a}{d}\right)\right] + \xi^2 \left(\frac{d}{2\pi h}\right)^{\gamma-1} 2^{\gamma} \Gamma^2\left(\frac{\gamma + 1}{2}\right) \sum_{n=1}^{\infty} \frac{\cos n\left(\frac{2\pi a}{d}\right)}{n^{1+\gamma}} \tag{26}$$

where $\Gamma(\mu)$ denotes the gamma function.

The roots of this dispersion equation were obtained by digital computer using an algorithm known as the bisection method [9]. This is an iterative procedure for establishing the interval containing the solution, to whatever degree of accuracy is required. The weighted integrals of the modified Bessel function, defined in (25), were determined by using a rapidly converging expansion in powers of u, thus taking advantage of the fact that $u < 1$.

III. Measurement of Phase Velocity

The variation of v/c as a function of frequency was determined experimentally by measuring the wavelength of the guided wave with the arrangement represented in Figure 3. The array was excited by a horn and turned through a bend of 180°, in the plane perpendicular to the elements, before entering the measurement section. This section consisted of a straight array of approximately 250 elements supported by a polyethelene tube. It was observed that the tube alone would not support any guided wave over the frequency range of interest, so that it may be considered to be transparent. The array was shunted by a highly reflective disk. The disk diameter was large enough so that almost all the power in the guided wave was intercepted, the result being a well-defined standing-wave pattern. The purpose of the 180° bend was to prevent any direct horn radiation from interfering with the measurements. With this arrangement the standing-wave ratios were

often as high as 40 dB, and the variance of wavelength measurements was well within the repeatability, indicating a single mode of propagation.

The measured values of v/c as a function of frequency are shown in Fig. 4 for arrays with an element length $2h$ of 1.5 cm and an interelement spacing d of 0.64 cm. The frequency range was between 5800 and 7000 Mc/s, the different sets of points corresponding to arrays of cylinders with different radii, as indicated. Superimposed on the experimental points are the theoretical values calculated from (23), using the particular values of γ which give what appears to be the best agreement with the measurements. The precision with which these values may be determined is attributed to the dependence of β on the second derivative of the current distribution, as noted earlier. It is significant, in view of this critical relationship between current density and propagation constant, that the assumed distribution of (18) accurately predicts the variation of phase velocity with frequency over the entire range of interest.

The discrepancies at the higher frequencies may be attributed largely to the failure of the approximation $\beta d \ll 2\pi$, since the wavelength of the slow wave may no longer be considered very large compared to the interelement spacing d. In addition, one must recognize that the actual current distribution, to which (18) is an approximation, also changes as the frequency is increased, placing a definite limitation on the range over which the assumed current distribution can be used.

In Figure 5 we have plotted the variation of γ with element radius, normalized to the half-length h. Our conjecture, which is made by analogy with a single isolated element [4], is that γ depends primarily on a/h, so that if a similar curve were plotted for a different interelement spacing, it would be almost coincident with the one shown here. The variation is essentially linear, with γ increasing from a value of approximately two for very thin elements. Since, over this frequency range, the parabolic distribution (with $\gamma=2$) is very close to the so-called shifted cosine distribution noted in (1), there is a consistency with previous research on the properties of thin linear antennas. We note also that γ is an increasing function of element radius, which means that thicker elements have a more uniform current distribution near the center with a steeper decrease to zero near the ends. This is to be expected, since for thicker elements the larger surface area at the ends will carry a correspondingly larger total charge. In using an equivalent filamentary element, we would then expect a larger effective linear charge density near the ends and, from the continuity equation.

$$\frac{\partial j}{\partial x} - i\omega\rho = 0, \tag{27}$$

a larger slope in the current distribution.

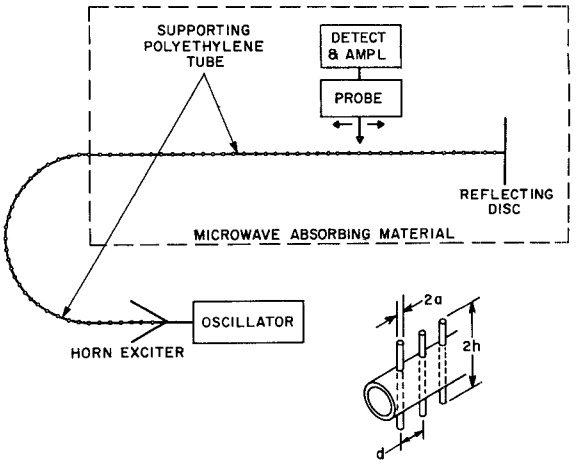

Fig. 3. Experimental arrangement for measuring wavelength. Elements are supported in polyethelene tube.

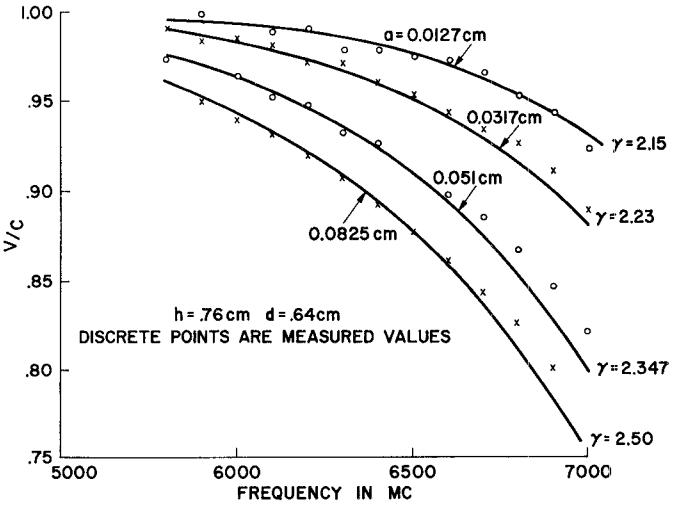

Fig. 4. Comparison between measured and theoretical values for v/c showing best estimates of γ.

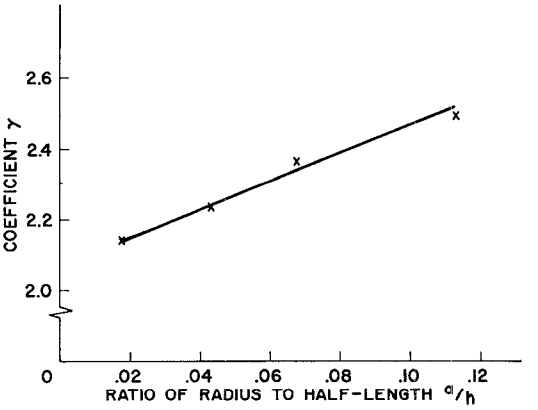

Fig. 5. Variation of γ with element radius a, normalized to half-length h.

IV. An Approximate Analysis Related to Yagi Antennas

In this section we derive an approximate solution to the dispersion equation for the limiting case of $v/c \approx 1$. This regime is of particular interest in the wave theory analysis of Yagi antennas since the closer v/c is to unity, the more loosely bound will be the slow wave and the larger the antenna "aperture." The result is based on the small argument behavior of $K_0(x)$, which is given by [8]

$$K_0(x) = -\log(Cx)[1 + O(x^2)] \tag{28}$$

where log C is related to Euler's number, $E \approx 0.5772 \cdots$, by the expression [10]

$$\log C = E - \log 2.$$

Using this approximate representation for K_0 in (23), we determine the root u as

$$u \approx \exp\left\{0.11593 - \frac{\gamma+1}{\gamma\xi^2} \cdot \left[A(\gamma) + \frac{\gamma}{\gamma+1} - \xi^2 + \frac{\xi^2}{(\gamma+1)^2}\right]\right\} \tag{29}$$

where the quantities on the right-hand side have been defined earlier.

In Fig. 6 we have compared approximate and exact solutions to the dispersion equation, for the thinnest element, $a = 0.0127$ cm. It is clear that v/c need not be significantly less than unity before there is a noticeable disagreement. This is due to the dependence of v/c on u, which is such that u increases so rapidly as v/c decreases that the logarithmic approximation to K_0 quickly becomes inadequate. Nevertheless, (29) can be useful in estimating v/c or providing a starting point for a more accurate calculation.

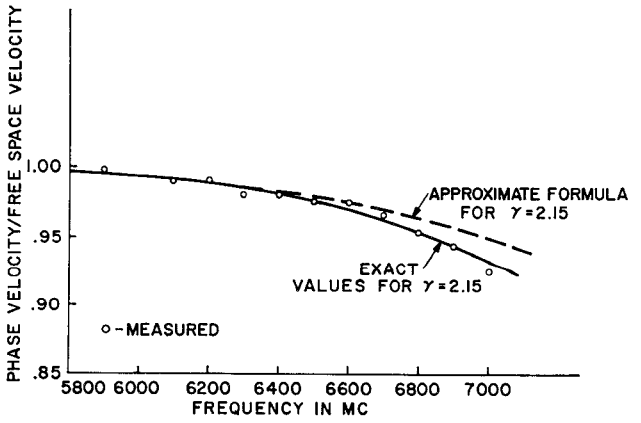

Fig. 6. Evaluation of approximate solution to dispersion equation for thinnest element, $a/h \approx .02$.

V. Summary and Conclusions

We have considered the characteristics of the lowest order slow wave which can propagate along an infinite array of parasitic linear elements. The investigation is empirical in the sense that we have assumed a model for the element current distribution including an undetermined parameter, which is later adjusted to give the best agreement between theoretical and measured values for phase velocity as a function of frequency.

We observe, just as in the case of linear antennas [3], that while the shifted cosine current distribution may be adequate to describe the behavior of very thin elements, a more uniform current is necessary for thicker cylinders in order to obtain agreement with the experimental results.

This is not to say that the current density departs very significantly from the parabolic distribution $\gamma = 2$, even for the thickest elements, since the largest value of γ was approximately $\gamma \approx 2.5$. However, since the propagation constant depends on the second derivative of $j(x)$, small errors become amplified in the estimate of β. We have, in this approach, exploited this behavior and, starting with accurate results for β, we have used the sensitivity to precisely determine the best one-parameter estimate for the current density.

Acknowledgment

The authors wish to acknowledge the contributions made by Miss Judith N. Hoffspiegel, who programmed the computations, and J. R. Donnell, who performed the measurements.

References

[1] R. Mailloux, "Antenna and wave theories of infinite Yagi-Uda arrays," *IEEE Trans. on Antennas and Propagation*, vol. AP-13, pp. 499–506, July 1965.
[2] J. Shefer, "Periodic cylinder arrays as transmission lines," *IEEE Trans. on Microwave Theory and Techniques*, vol. MTT-11, pp. 55–61, January 1963.
[3] F. Serracchioli and C. A. Levis, "The calculated phase velocity of long end-fire uniform dipole arrays," *IEEE Trans. on Antennas and Propagation*, vol. AP-7, spec. suppl., pp. S424–S434, December 1959.
[4] R. W. P. King, *Theory of Linear Antennas*. Cambridge, Mass.: Harvard University Press, 1956.
[5] P. M. Morse and H. Feshbach, *Methods of Theoretical Physics*. New York: McGraw-Hill, 1953, p. 467.
[6] A. Erdélyi, Ed., *Tables of Integral Transforms*, vol. 1. New York: McGraw-Hill, 1954, p. 17.
[7] J. C. Slater, *Microwave Electronics*. Princeton, N. J.: Van Nostrand, 1950, p. 170.
[8] See, for example, S. Schelkunoff, *Electromagnetic Waves*. Princeton, N. J.: Van Nostrand, 1943, p. 369.
[9] R. W. Hamming, *Numerical Methods for Scientists and Engineers*. New York: McGraw-Hill, 1962, p. 352.
[10] A. Erdélyi, Ed., *Higher Transcendental Functions*, vol. II. New York: McGraw-Hill, 1953, ch. 7.